# A FRAMEWORK FOR IMAGE MAGNIFICATION: INDUCTION REVISITED

*Laurent Condat and Annick Montanvert*

Laboratoire LIS – Fédération ELESA
961, rue de la Houille Blanche – BP 46
38402 Saint Martin d'Hères cedex, France
E-mail: laurent.condat@lis.inpg.fr

**ABSTRACT**

An original image magnification method called *induction* was proposed recently [1], whose specificity is to state the problem of image magnification as an inverse problem of image reduction. The methods usually employed, like interpolation, fail to verify this constraint, which provides a formalism for magnification and a framework for evaluating the quality of the enlarged images. In this paper, we revisit the induction through a new interpretation using wavelets. We put forward major improvements including a direct implementation, much more efficient than the iterative algorithm proposed previously.

## 1. MOTIVATION

Image magnification is required in many facets of image processing, such as still photographs zooming. The problem consists in increasing the resolution of a digital image by using *a priori* knowledge on the scene underlying the image. The frequency content, available in the initial image, is fundamentally limited by the sampling theorem, which can be defeated if a model is able to predict the missing high frequencies needed to reconstruct the edges in the enlarged image.

Linear magnification methods, whose best known representative is spline interpolation [2], fail to add in extra details, and artifacts like blurring or ringing show up. Many nonlinear interpolation techniques (e.g. [3, 4]) have been proposed, which estimate the localization of existing edges with subpixel accuracy, and synthesize them at the higher resolution. They produce pleasant images, but there is no clear relationship ensuring coherence between the initial and the enlarged images.

A solution to this problem was proposed in [1], with a method called *induction*: a process has been defined to regularize the enlarged image, obtained with whatever magnification method, in order to restore the information lost during the enlargement, but present in the initial image. To this end, *magnification is stated as an inverse problem of reduction*: the enlarged image should, when reduced, give back the initial image. This principle was also adopted in other works like [5] and [6], which always amount to optimize a likelihood criteria under constraint, whereas we use a more general and more efficient set-theoretic approach.

In this paper, we redefine the induction through a new formalism which provides a framework for image resizing and gives strong fundations to the method. A fast implementation and a generalization called *oblique induction* are proposed and explained through the wavelet theory.

## 2. PRINCIPLES OF IMAGE RESIZING

In order to resize a digital image $I = (I[k,l])_{(k,l)\in\mathbb{Z}^2}$, its formation process needs to be hypothesized. If the pixels $I[k,l]$ are samples of an underlying scene $f(x,y)$ continuously defined, i.e. $I[k,l] = f(x,y)|_{x=k,y=l}$, then interpolation is well-suited for magnification: one only has to estimate a function that goes through the pixel values, and resample it on a finer grid. Such a model is not realistic for natural images: since $f$ is not bandlimited, $I$ would be polluted by aliasing with such a formation process.

Therefore we adopt a more appropriate model, where a digital image is produced by an imaging device with point-spread-function (PSF) $\Gamma(x,y)$. The acquisition is supposed free of noise, and can be modeled by a convolution followed by sampling:

$$I[k,l] = f * \Gamma\,(k,l), \quad (k,l) \in \mathbb{Z}^2. \tag{1}$$

Now we define $I^{(\alpha)}$, the resized version of $I$ by a factor $\alpha$, as the image provided by the same imaging device if the scene $f$ had been dilated by a factor $\alpha$ in each direction, that is

$$I^{(\alpha)}[k,l] = \big(f(\alpha\bullet,\alpha\bullet) * \Gamma\big)\,(k,l) \tag{2}$$

$$= \frac{1}{\alpha^2}\big(f * \Gamma(\bullet/\alpha,\bullet/\alpha)\big)\,(\alpha k,\alpha l). \tag{3}$$

Here $\alpha > 1$ corresponds to a reduction, $\alpha < 1$ to a magnification. In this paper we only deal with the case where $\alpha$ is an integer, denoted $a$. Now let us assume that $\Gamma(x,y)$ verifies a two-scale relation with integer dilation factor $a \geq 2$:

$$\Gamma(x/a, y/a) = a^2 \sum_{(k,l)\in\mathbb{Z}^2} R[k,l]\,\Gamma(x-k, y-l). \tag{4}$$

Combining Eqns. (3) and (4) provides us with the way to reduce an image by an integer factor $a$: reducing simply consists in discrete filtering followed by downsampling, which is defined by the operator $[I]\downarrow a = \big(I[ak,al]\big)_{(k,l)\in\mathbb{Z}^2}$, that is to say

$$I^{(a)} = [\,I * R\,]\downarrow a. \tag{5}$$

This is the usual way for reducing an image, here derived through the proposed image model. The Shannon theorem is verified *a posteriori*, if $\Gamma$ (then $R$) is lowpass, which is the case with most practical imaging devices. Practically, $\Gamma$ is often unknown, then $R$ must be chosen directly with good properties [7].

Note that this formalism is nothing else than the basic principle of the multiresolution theory [8]: whatever the resolution, the image pixels are scalar products of the scene with dilates and translates of a single prototype $\Gamma$. The reduction also amounts to the lowpass analysis in a wavelet decomposition.

Given an image $I$, the problem of its magnification is still open because $f$ is unknown, then Eqn. (3) is of no help. But according to our formalism, a magnification followed by a reduction with the same factor is a lossless process: the enlarged image $I^{(1/a)}$, when reduced, gives back the initial image:

$$[\, I^{(1/a)} * R\,] \downarrow a = I. \tag{6}$$

This condition, called the *reduction constraint*, leads naturally to state the magnification operation as a pseudo-inverse of the reduction, as we do in the next sections.

## 3. INDUCTION IN ITS ORIGINAL FORM

Image magnification is an ill-posed problem. Given an initial image $I$ and a reduction filter $R$, there is a whole set, called *the induced set* $\Omega$, of enlarged images verifying the reduction constraint:

$$\Omega = \{X \;\mid\; [\, X * R\,] \downarrow a = I\}. \tag{7}$$

The true enlarged image $I^{(1/a)}$ must be estimated among $\Omega$. For this purpose, let us consider a visually pleasing enlarged image $J$, which does not verify the reduction constraint. $J$, called the *inducing image*, can be obtained with any magnification method, e.g. interpolation. The induction simply consists in projecting orthogonally $J$ onto $\Omega$, so as to obtain an *induced image* $K$ which belongs to $\Omega$, as illustrated in fig. 1.

The method proposed in [1] uses *projection onto convex sets* (POCS) techniques [9], consisting in expressing each condition on the enlarged image to be constructed, as a convex constraint set $\Omega_{k,l}$ in the image space. Then an image lying in the intersection $\Omega = \bigcap_{(k,l)\in\mathbb{Z}^2} \Omega_{k,l}$ of all constraint sets, is a solution of the problem. Here each $\Omega_{k,l}$ is the set of enlarged images that satisfy the reduction constraint at pixel $(k, l)$. It is the affine space

$$\Omega_{k,l} = \{X \;\mid\; X * R\,[ak, al] = I[k, l]\}. \tag{8}$$

In its original form, the induction is an iterative algorithm: during the $(n+1)$th iteration, the image $J_n$ is updated in place by successive projections onto each $\Omega_{k,l}$

$$J_{n+1} = \mathrm{Proj}_{\Omega_{N-1,M-1}} \circ \cdots \circ \mathrm{Proj}_{\Omega_{0,1}} \circ \mathrm{Proj}_{\Omega_{0,0}}\,(J_n), \tag{9}$$

where $I$ is supposed of size $N \times M$, and $J_0 = J$ is the inducing image. The induced image $K = J_\infty$ is obtained at convergence. The choice of the operator $\mathrm{Proj}_{\Omega_{k,l}}$ is detailed in [1].

Thus the induction provides the image in $\Omega$ which is the closest to $J$ in the $\ell_2$ sense (and, to some extent, in the visual sense). The induction acts as a post-processing, regularizing the inducing image so that it is in accordance with our image formation model, through the reduction constraint. The choice of the inducing image is therefore crucial, as we will show in section 6.

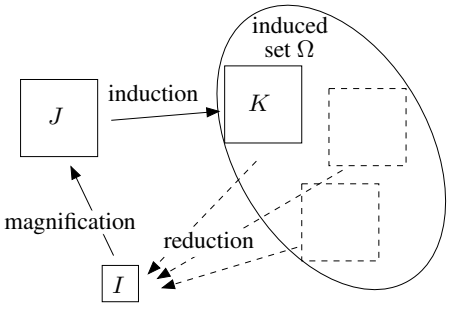


**Fig. 1**. Induction principle.

## 4. FAST INDUCTION

Before generalizing the induction process, we present in this section a major improvement, which is a non-iterative, therefore much faster, implementation of the induction method. To this end, let us go back to the principle behind the iterative method: the difference between $I$ and the reduced version of $J$ is back-propagated in $J$. This can be implemented as depicted on the following flow-graph:

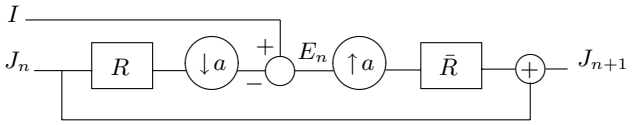


where we used the reversion : $\bar{R}[k, l] = R[-k, -l]$. The convergence to $K$ is ensured, albeit slower than with the POCS methods, which only optimize the way the correction is done during each iteration. Now if we note $E = \sum_{n\in\mathbb{N}} E_n$ and introduce the upsampling operator $[\,\cdot\,]\uparrow a$ which inserts $a-1$ zeros between each sample in each direction, we get

$$K = J + [\, E\,]\uparrow a * \bar{R}. \tag{10}$$

$K$ verifies the reduction constraint, then

$$\begin{array}{ll} & [\, K * R\,] \downarrow a = I \\ \Leftrightarrow & [\, (J + [\, E\,]\uparrow a * \bar{R}) * R\,] \downarrow a = I \\ \Leftrightarrow & [\, J * R\,] \downarrow a + E * [\, \bar{R} * R\,] \downarrow a = I \\ \Leftrightarrow & E = (I - [\, J * R\,] \downarrow a) * ([\, \bar{R} * R\,] \downarrow a)^{-1}. \end{array} \tag{11}$$

Hence K can be computed directly, simply by inserting, before the upsampling step, the inverse filter $C^{-1} = ([\, \bar{R} * R\,] \downarrow a)^{-1}$ which cancels the correlation between $R$ and its $a-$translates:

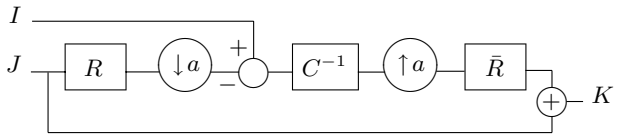


This fast implementation will allow us to generalize the induction in the following section.

## 5. OBLIQUE INDUCTION

We can now improve the induction process, by allowing the projection of the inducing image onto the induced set to be oblique, and not necessarily orthogonal any more. This yields

$$K = J + [\, I - [\, J * R\,] \downarrow a\,]\uparrow a * A, \tag{12}$$

where $A$ is a *biorthogonal partner* (see [10]) of $R$, i.e. a filter that verifies $[\, A*R\,] \downarrow a = \delta_{(0,0)}$, with $\delta_{(k,l)}[k, l] = 1$ and $\delta_{(k,l)}[i, j] = 0$ if $i \neq k$ or $j \neq l$. The oblique induction is implemented as:

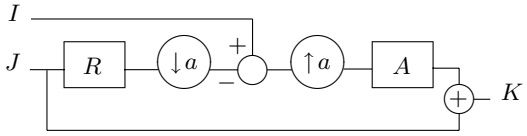

The orthogonal induction is a particular case where $A = \tilde{R}$ is the *dual filter* of $R$

$$\tilde{R} = \big([[\,\bar{R} * R\,]\downarrow a]\uparrow a\big)^{-1} * \bar{R} = [\,C^{-1}\,]\uparrow a * \bar{R}. \qquad (13)$$

This dual filter is not necessarily the best biorthogonal partner of $R$. Our experiments indicate that a better choice for most of images, whatever the filter $R$, is based on the cubic splines, whose interest for image processing is well known [2]. This corresponds to the choice

$$A = \big([[\,B_3 * R\,]\downarrow a]\uparrow a\big)^{-1} * B_3, \qquad (14)$$

where $B_3$ is obtained by sampling the centered cubic B-spline $\beta_3(x, y)$ (see [2]) with step $1/a$: $B_3[k, l] = \beta_3(k/a, l/a)$.

From this point, we will consider that all the filters are separable. Thus we adopt 1-D notations for the filters. For example, for a magnification by a factor $a = 2$, $B_3 = [\frac{1}{48}, \frac{1}{6}, \frac{23}{48}, \frac{2}{3}, \frac{23}{48}, \frac{1}{6}, \frac{1}{48}]$.

The freedom in the choice of $A$ provided by the oblique induction allows to perform the whole process only with FIR filters, without involving any inverse filter. If for example $R$=D9 from the D9/D7 pair used in JPEG2000 [11], $A$=D7 is a relevant choice.

The role of $A$ will be detailed in the next section.

## 6. INTERPRETATION IN TERMS OF WAVELETS

Eqn. (12) shows the induction as a regularization of the inducing image. The lowpass component of $J$ is indeed discarded and replaced by $I$: the induction consists in correcting the low-frequency part of the inducing image, while keeping its high-frequency part. Eqn. (12) can be rewritten under the more interesting form:

$$K = \underbrace{J - [\,[\,J * R\,]\downarrow a\,]\uparrow a * A}_{H} + \underbrace{[\,I\,]\uparrow a * A}_{L}. \qquad (15)$$

In other terms, the induced image is equal to $L = [\,I\,]\uparrow a * A$ plus a high-frequency image $H$ corresponding implicitly to the synthesis of the wavelet coefficients of $J$ at the finest resolution, as illustrated in Fig. 2 (with $a = 2$). The induced set can now be characterized more precisely: it is the affine space

$$\Omega = \{\tilde{L} + H \mid H \in V_R^{\perp}\} = \{L + H \mid H \in V_R^{\perp}\}, \qquad (16)$$

where $V_R = \mathrm{Vect}\big((R * \delta_{ak})_{k\in\mathbb{Z}}\big)$ is the vector space generated by $R$ and its $a-$translates, and $\tilde{L}$ is the image $I$ linearly enlarged with the dual of $R$ (see Eqn. (13)): $\tilde{L} = [\,I\,]\uparrow a * \tilde{R}$.

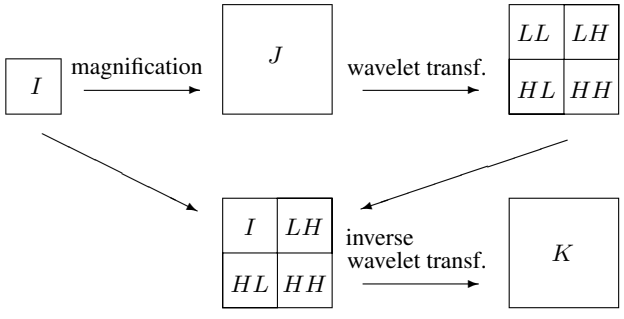


**Fig. 2**. Wavelet interpretation of the induction.

Among $\Omega$, $\tilde{L}$ is the image with minimal $\ell_2$ norm. If the oblique induction is performed, $A \neq \tilde{R}$, and $L$ can be interpreted as $L = \tilde{L} + \tilde{H}$ where $\tilde{H} \in V_R^{\perp}$ is the part of high frequencies which can be *linearly* predicted from $I$. If this prediction is good, that is $A$ is chosen correctly, the high frequencies that are added in during the induction itself (under the form of the image $H$) cannot be predicted linearly from $I$. Ideally, $H$ should be the *intrinsicly nonlinear* high frequencies that lack in $L$ in order for the enlarged image to have a good quality, particularly near edges, where a linear magnification will necessary fail to give enough sharpness.

These notions are summarized in Fig. 3. Clearly, the role of the inducing image $J$ is crucial. The considerations above indicate that $J$ must be obtained from $I$ by *nonlinear* magnification, creating coherent high frequencies for a good rendering of edges. The induction takes care of the low frequencies, by regularizing $J$ so that it belongs to the induced set.

We can further notice that:

- if the inducing image is uniform (e.g. all pixels to zero), no high frequency is brought, and $K = L$.
- if the inducing image is obtained by linear magnification from $I$: $J = [\,I\,]\uparrow a * B$, with $B$ not a biorthogonal partner of $R$, say by interpolation, one can calculate a filter $C$ so that $K$ can be computed directly, without using the induction process, by $K = [\,I\,]\uparrow a * C$. Moreover, $C \neq A$ so all the efforts for carefully designing the filter $A$ are in vain, because $L = [\,I\,]\uparrow a * A$ is the best we can do for predicting the high frequencies linearly.

As we have shown, the induction process combines the best of two worlds: the information available in $I$ is synthesized linearly at the higher resolution, and the required high-frequency details are created heuristically by the inducing magnification method. Therefore, the whole process can be interpreted as a nonlinear extrapolation in the wavelet domain.

## 7. RESULTS

Fig. 4 illustrates the good results obtained by oblique induction. A large factor $a = 4$ is employed so that the differences between the images are highly visible. The inducing method of Jensen *et al.* [3] is used, as well as $R = [\,D9\,]\uparrow 2{*}D9$ and $A = [\,D7\,]\uparrow 2{*}D7$. The nearest neighbor interpolated image is provided to show the information available in the initial image. The image $L$ suffers from a staircase effect due to the separability of the linear enlargement, and from ringing and blurring artifacts due to the lack of high frequencies. On the other hand, the image $J$ is pleasing, in spite of the painting effect due to the distortion of the low frequencies. $K$

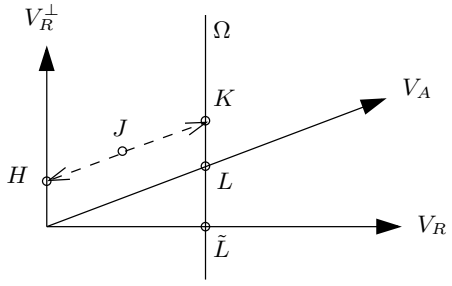


**Fig. 3**. Oblique induction in terms of projections.

is free from these artifacts, and is coherent with $I$. See in particular the details of the camera, which have almost disappeared in $J$, and are restored in $K$.

To validate the induction numerically, we propose to reduce an image $O$, so as to obtain an image $I$ which is enlarged by oblique induction and then compared to $O$, using $a = 2$, $R = D9$, $A = D7$. This yields the PSNR results shown in Tab. 1 for several well-known images. Two inducing methods have been tested: the magnification of Jensen *et al.*, and the nonlinear interpolation of Ramponi *et al.* [4]. The first column gives the PSNR for the image $L$, corresponding to a uniformly black inducing image (which is also the image $O$ passed through the lowpass analysis/synthesis branch of the D9/D7 biorthogonal filterbank).

The numerical results are in accordance with the visual quality: the large differences between $K$ and $L$ with both inducing methods shows that the prediction of the finest wavelet coefficients is efficient, in particular with the method of Jensen. This suggests to use the induction as a framework for evaluating the quality of the magnification methods in the literature, as will be done in future work. Note that using $A = \tilde{R}$ instead of $D7$ leads to an average penalty of $0.1$ dB for the induced images, whereas the spline filter of Eqn. (14) yields an average improvement of $0.05$ dB.

There is another potential application in resolution-scalable lossless image coding: as it acts like an extrapolation in the wavelet domain, the induction can be seen as an additional prediction step in an implementation based on the lifting scheme.


**Fig. 4**. Part of *camera* image enlarged by a factor of 4.

| image | black $K = L$ | Ramponi $J$ | Ramponi $K$ | Jensen $J$ | Jensen $K$ |
|---|---|---|---|---|---|
| Lena | 35.26 | 34.51 | 35.14 | 33.34 | **35.50** |
| Baboon | 24.50 | 24.13 | 24.44 | 23.46 | **24.64** |
| Lighthouse | 26.77 | 26.24 | 26.72 | 26.02 | **27.12** |
| Camera | 26.96 | 26.79 | 27.22 | 26.22 | **27.51** |
| Peppers | 33.47 | 34.45 | **34.85** | 32.99 | 34.46 |
| Bike | 26.39 | 26.51 | 27.19 | 25.97 | **27.41** |
| Cafe | 23.60 | 23.25 | 23.81 | 22.49 | **24.05** |

**Table 1**. Images reduced then magnified ($a = 2$), compared with their original counterparts, without ($J$) and with ($K$) induction.

## 8. CONCLUSION

In this paper, we proposed a fast implementation, a generalization, and a better understanding of the induction process. The method is flexible, through the choice of the filters and of the inducing magnification method, for which we proposed practical examples. The formalism introduced justifies the use of induction, in comparison with traditional magnification methods. We currently continue our work on the choice of the inducing method and on the extension to non-integer magnification factors.

## 9. REFERENCES


[1] D. Calle and A. Montanvert, "Super-resolution inducing of an image," in *Proc. of ICIP*, 1998, pp. 232–236.

[2] M. Unser, "Splines: A perfect fit for signal and image processing," *IEEE Signal Proc. Mag.*, vol. 16, no. 6, 1999.

[3] K. Jensen and D. Anastassiou, "Subpixel edge localization and the interpolation of still images," *IEEE Trans. Image Proc.*, vol. 4, no. 3, pp. 265–295, Mar. 1995.

[4] G. Ramponi and S. Carrato, "Interpolation of the DC component of coded images using a rational filter," in *Proc. of ICIP*, 1997, pp. 389–392.

[5] R. R. Schultz and R. L. Stevenson, "A Bayesian approach to image expansion for improved definition," *IEEE Trans. Image Proc.*, vol. 3, no. 3, pp. 233–242, May 1994.

[6] H. Aly and E. Dubois, "Regularized image up-sampling using a new observation model and the level set method," in *Proc. of ICIP*, 2003, pp. 665–668.

[7] P. J. Burt and E. H. Adelson, "The Laplacian pyramid as a compact image code," *IEEE Trans. Communications*, vol. 31, no. 4, pp. 532–540, Apr. 1983.

[8] S. Mallat, "A theory for multiresolution signal decomposition: The wavelet representation," *IEEE Trans. Pat. Anal. Mach. Intell.*, vol. 11, no. 7, pp. 674–693, July 1989.

[9] D. C. Youla and H. Webb, "Image restoration by the method of convex projections: Part 1 - theory," *IEEE Trans. Medical Imaging*, vol. MI-1, no. 2, pp. 81–94, Oct. 1982.

[10] P. P. Vaidyanathan and B. Vrcelj, "Biorthogonal partners and applications," *IEEE Trans. Signal Proc.*, vol. 49, no. 5, pp. 1013–1027, May 2001.

[11] M. Antonini, M. Barlaud, P. Mathieu, and I. Daubechies, "Image coding using wavelet transformation," *IEEE Trans. Image Proc.*, vol. 1, no. 2, pp. 205–220, Apr. 1992.